View metadata, citation and similar papers at core.ac.uk

brought to you by CORE

provided by Aston Publications Explorer

© 2016, Elsevier. Licensed under the Creative Commons Attribution-NonCommercial-NoDerivatives 4.0 International
http://creativecommons.org/licenses/by-nc-nd/4.0/

Molecular alignment relaxation in polymer optical fibers for sensing applications

Pavol Stajanca[1,*], Onur Cetinkaya[2], Marcus Schukar[1], Pawel Mergo[2], David J. Webb[3], Katerina Krebber[1]

[1] BAM Federal Institute for Materials Research and Testing, Unter den Eichen 87, D-12205 Berlin, Germany
pavol.stajanca@bam.de (P.S.), marcus.schukar@bam.de (M.S.), katerina.krebber@bam.de (K.K.)

[2] Marie Curie-Sklodowska University, Pl. M. Curie-Sklodowskiej 3, 20-031 Lublin, Poland
onur.cetinkaya@poczta.umcs.lublin.pl (O.C.), pawel.mergo@poczta.umcs.lublin.pl (P.M.)

[3] Aston Institute of Photonic Technologies, Aston University, Aston Triangle, Birmingham, B4 7ET, UK
d.j.webb@aston.ac.uk (D.J.W.)

Abstract: A systematic study of annealing behavior of drawn PMMA fibers was performed. Annealing dynamics were investigated under different environmental conditions by fiber longitudinal shrinkage monitoring. The shrinkage process was found to follow a stretched exponential decay function revealing the heterogeneous nature of the underlying molecular dynamics. The complex dependence of the fiber shrinkage on initial degree of molecular alignment in the fiber, annealing time and temperature was investigated and interpreted. Moreover, humidity was shown to have a profound effect on the annealing process, which was not recognized previously. Annealing was also shown to have considerable effect on the fiber mechanical properties associated with the relaxation of molecular alignment in the fiber. The consequences of fiber annealing for the climatic stability of certain polymer optical fiber-based sensors are discussed, emphasizing the importance of fiber controlled pre-annealing with respect to the foreseeable operating conditions.

Keywords: Polymer optical fibers, optical fiber sensor climatic stability, thermal annealing, molecular alignment relaxation, humidity induced annealing.

1. Introduction

Following the success in short range data transmission applications [1], polymer optical fibers (POFs) have attracted considerable attention also in the field of optical fiber sensors [2]. Building on well recognized advantages of silica fiber sensors such as low-weight, compactness or electromagnetic immunity, POF-based sensors may represent lower cost or superior performance alternatives, in certain applications. One of the key motivations for using polymer materials relates to their mechanical properties. Polymer optical fibers can exhibit much higher elasticity, ductility and bending flexibility than their glass counterparts, which make them attractive especially for strain sensing applications. However, the polymer fiber mechanical properties are strongly dependent on molecular alignment in the fiber. The fiber drawing process causes rearrangement of polymer molecules that tend to align along the fiber axis. Quantification of molecular alignment degree in the fiber is a non-trivial task as it dependents on various drawing conditions and the thermal history of the fiber preform. Nevertheless, its influence on the mechanical [3–6] and optical properties [7,8] of drawn polymer fibers has been clearly shown.

Molecular alignment can be also viewed in terms of residual stress frozen in the fiber after the drawing process. As such, it is subject to thermal relaxation resulting in a change of the fiber mechanical properties [6]. Moreover, this annealing process is accompanied by the permanent longitudinal shrinkage and diameter increase of the fiber. Thermal annealing can thus have a detrimental effect on

* Corresponding author

various fiber properties, such as the modal character or optical losses [9], that need to be considered with respect to fiber climatic stability in general. For certain fiber sensing methods, such as fiber Bragg grating (FBG) or interferometric sensors, fiber longitudinal shrinkage itself might be the most obvious and severe issue since the sensor reading is directly tied to the longitudinal coordinate in the fiber in some way (Bragg wavelength, resonator length). The issue was recognized in the sensing community to some extent. Nowadays, most of the authors perform short term fiber annealing in order to remove residual stress and avoid the fiber shrinkage later during the sensor operation [10,11]. Annealing does not need to be necessarily of a detrimental nature. It can be used for controlled post-inscription down-tuning of FBGs to a desired wavelength or to inscribe wavelength multiplexed FBGs with a single phase-mask [12]. Even though the basic effects and role of fiber annealing earned a partial recognition, no deeper study of the annealing process was carried out up to now.

The climatic stability and reliability of POF-based sensors is an important topic for their further practical implementation. In this work, we therefore present a thorough investigation of the annealing behavior of drawn polymer fibers revealing complexity of the annealing process. Besides dependence on the initial molecular alignment in the fiber, temperature and time, also a strong influence of humidity on the fiber annealing behavior was shown for the first time. Results obtained for various fiber samples and annealing conditions show an underestimation of annealing dynamics in previous works. In addition, the annealing study provides a useful insight into the molecular structure of fibers, pinpointing the heterogeneous nature of molecular dynamics in polymer systems. Finally, the influence of annealing on the fiber mechanical properties is briefly considered as well.

2. Fiber samples

A variety of large-core multi-mode (MM) POFs from different materials is nowadays available commercially. On the other hand, there is a general lack of quality single-mode (SM) polymer fibers required for high-precision sensing applications. Experimental SM POFs are being produced by various research groups with the vast majority of them relying on a microstructured fiber architecture [13]. The most common method for preparing microstructured POFs (mPOFs) is by drilling a periodic array of air holes of desired geometry along the axis of a bulk polymer rod that is subsequently drawn into the fiber. For simplicity, the work described in this paper was performed with homogeneous fibers without any microstructure. For the usual 125 μm diameter SM mPOF, the cross-sectional area of the air fraction is typically lower than 1% of the total area and so the microstructured region is not expected to have significant influence on the fiber straining or annealing behavior. Our study focusses on fibers drawn from polymethyl methacrylate (PMMA), as it is the most common material for POF fabrication up to now. However, it is reasonable to expect that most qualitative findings should be applicable to a wider range of polymer materials.

All fiber samples were prepared from commercial PLEXIGLASS® XT rod with a diameter of 30 mm from Evonik Industries AG [14]. Here we note that we use the same PMMA rod type only with larger diameter for fabrication of our standard mPOFs by the preform drilling method [15]. The level of induced molecular alignment is a complex function of various drawing conditions, where fiber drawing stress is the key pointer for determining the alignment degree. For the purposes of this work we prepared three fiber samples drawn under different drawing force with the same target diameter between 200 μm and 250 μm. Samples were fabricated from the same preform in a single pull process by varying the drawing temperature. The not fully optimized drawing process for our experimental SM

mPOFs typically yields fibers with higher diameter fluctuations than the more mature production of silica fibers or MM POFs. Diameter fluctuations translate also into the degree of molecular alignment in the fiber and may therefore compromise discrimination between individual samples. In order to overcome this problem, we decided to prepare only three fibers but with significantly different drawing conditions. An oven temperature of 215 ^{o}C resulted in a rather high drawing force of 0.8 N, while increasing temperature to 290 ^{o}C yielded a drawing force at the detection limit of our load cell. For labeling purposes in the rest of the work, we will refer to this fiber as drawn under 0 N. In addition, fiber drawn at an intermediate 0.4 N (240 ^{o}C) was added to closer match typical drawing conditions that we normally use for mPOFs.

3. Annealing procedure

Molecular alignment is a non-equilibrium state frozen in the fiber as it cools down after exiting the heating oven. It is subject to thermal relaxation when aligned molecules are trying to return to their equilibrium state of randomly oriented entanglement. This change in molecular organization manifests itself by change in geometrical, mechanical as well as optical properties. Different fiber parameters can be thus used to investigate this process, but monitoring of fiber longitudinal shrinkage is the most straightforward one. Samples of all three fiber types with an initial length of 50 cm were annealed inside the climate chamber at the same time in order to ensure the same conditions and comparable results. Samples were freely lying on a thick piece of cardboard to insulate them from a metal grid of the climate chamber that might act as a heat sink and distort the measurement, especially for short annealing times. A relatively long length of 50 cm was chosen in order to minimize the uncertainty associated with fiber length measurement. At the same time, it is short enough, so the fibers can be freely placed into the climate chamber without interfering with each other, as this might prohibit their shrinkage. Moreover, annealing of longer samples provides inherent averaging with respect to fiber diameter fluctuations along the sample.

All annealing experiments were performed utilizing a Vötsch VCL 4006 climate chamber enabling programmable control of temperature and relative humidity (RH). PMMA, along with many other polymers, exhibit affinity for water. Diffusion of water into polymer fibers is a relatively slow entropy-driven process dependent on the relative humidity of the environment. At the beginning of each annealing cycle (Figure 1), fibers are firstly held inside the climate chamber for one hour at initial temperature T_{In} = 21.4 ^{o}C and target humidity H_{An} in order to allow water diffusion into the fiber. Temperature is then gradually increased (1 hour ramp) to target value T_{An} at which the fibers are held for certain annealing time interval t_{an}. Subsequently, fibers are rapidly cooled back to T_{In}, where they are kept for 2 hours to stabilize. The relative humidity value remains the same for the whole annealing cycle. The fibers are removed from the climate chamber and left for a minimum of 2 hours to stabilize at room conditions (20-24 ^{o}C and 30-40 % RH). The length of all the samples is measured after each cycle and annealing process is repeated for the same samples with gradually increasing t_{An} until no further significant shrinkage of fiber is observed. The fiber annealing dynamics is then evaluated in terms of temporal evolution of the relative fiber length at given annealing conditions. The whole annealing procedure is repeated with new samples for the different sets of environmental conditions.

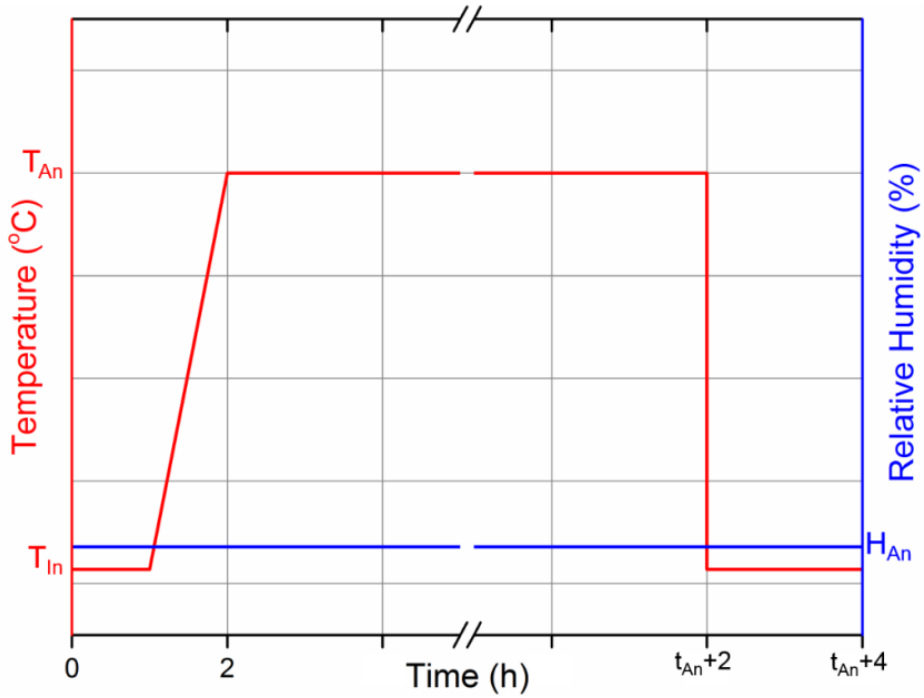

Figure 1. Schematic diagram of one annealing cycle in the climate chamber.

4. Mechanical testing

In order to assess the influence of fiber annealing on its mechanical properties, a fiber strain test was performed for original un-annealed, as well as selected annealed samples. Strain testing was performed on in-house built tensile testing machine comprising of one static fiber holder with load cell for measuring the force and one stepper-motor-driven traveling crosshead with a linear displacement sensor for fiber straining. The ends of 5 cm long fiber samples were glued to the fiber holders yielding an initial fiber gauge length of approximately 20 mm. Based on an actual gauge length measurement, fiber straining rate was always adjusted to be in 66-67 %/min range. Sample initial diameter was measured by micrometer screw gauge at 3 different points along the strained length of the fiber.

5. Results and discussion

5.1 Annealing dynamics and molecular alignment

During our studies, samples with the different degree of initial molecular alignment were annealed under various environmental conditions. In order to investigate the basic annealing dynamics and the role of the fiber initial molecular alignment, we used data obtained from experiments at 95 °C and 40 % RH. This corresponds to the highest annealing temperature allowing simultaneous humidity control in our climate chamber. At the same time, it is still well below the glass transition temperature (T_g) of used PMMA, which was measured to be between 105 °C and 115 °C for the bulk isotropic material. As discussed later, higher temperature is associated with a larger degree of shrinkage, which makes the illustrated effects more apparent. Nevertheless, general trends that we will describe in this section hold also at the different annealing conditions. Utilization of longer (50 cm) samples provides a certain degree of inherent averaging with regard to short-distance fiber properties fluctuations. Additionally, in this case we annealed three samples from different regions of each fiber type in order to

account also for possible long-distance fluctuations. The presented data are then average from 3 samples for each fiber type.

An attempt has been made to model fiber shrinkage by simple exponential decay [6], which is typical for the relaxation of many physical systems. In our study, however, we found that fiber shrinkage follows a stretched exponential decay function rather than simple exponential decay. Figure 2a depicts the temporal evolution of the relative length *L* of the fiber drawn under 0.4 N during a 312 hour-long annealing cycle. For illustration, measured data are fitted by both, stretched and simple exponential decay functions of the form

$$L = L_0 + L_{An} e^{-(\frac{t}{t_0})^g},$$

where L_0 represents the limiting fiber length to which fiber shrinkage converges at the certain annealing temperature, L_{An} is the magnitude of the total inducible shrinkage at that temperature, t is the annealing time, t_0 is the fundamental decay time and $0 < g \leq 1$ is the stretching parameter. In the case of simple exponential decay, $g = 1$. Stretched exponential decay can be interpreted as a superposition of a group of simple exponential decay functions with a nontrivial distribution of decay times. The stretching parameter g is associated with the width of the decay time distribution and is a measure of heterogeneity of the studied system. The lower g gets, the more heterogeneous (broader) is the decay time distribution [16]. Heterogeneous dynamics are characteristic of disordered systems and have been a hot topic in the field of supercooled liquids in the last decades [17,18]. The nature and origins of heterogeneous dynamics in polymers are still not fully understood, but are often attributed to microscopic heterogeneities in the molecular arrangement of the material. Polymer material can be imagined as a mass of loosely entangled strings representing polymer molecules. Different microscopic regions might have different degrees of entanglement, which in turn affects their mobility. Fiber annealing studies can therefore shed some light on the mechanism of molecule alignment and its consequences for the material properties, which are not fully understood [19]. To illustrate the magnitude and importance of heterogeneous dynamics for the fiber annealing process, the fitted parameters are summarized in Table 1. However, relaxation time analysis from discrete annealing data is of ill-conditioned nature and thus very sensitive to the precision of experimental data and truncation effects [20]. We will therefore avoid any rigorous quantitative analysis of the fitted parameters, which goes beyond the scope of this work. Rather than that, we will use our findings to point out and discuss the qualitative consequences of the heterogeneous nature of the material on the annealing process and climatic stability of drawn polymer fibers. Stretched exponential decay fits of experimental data will be included for eye guidance only.

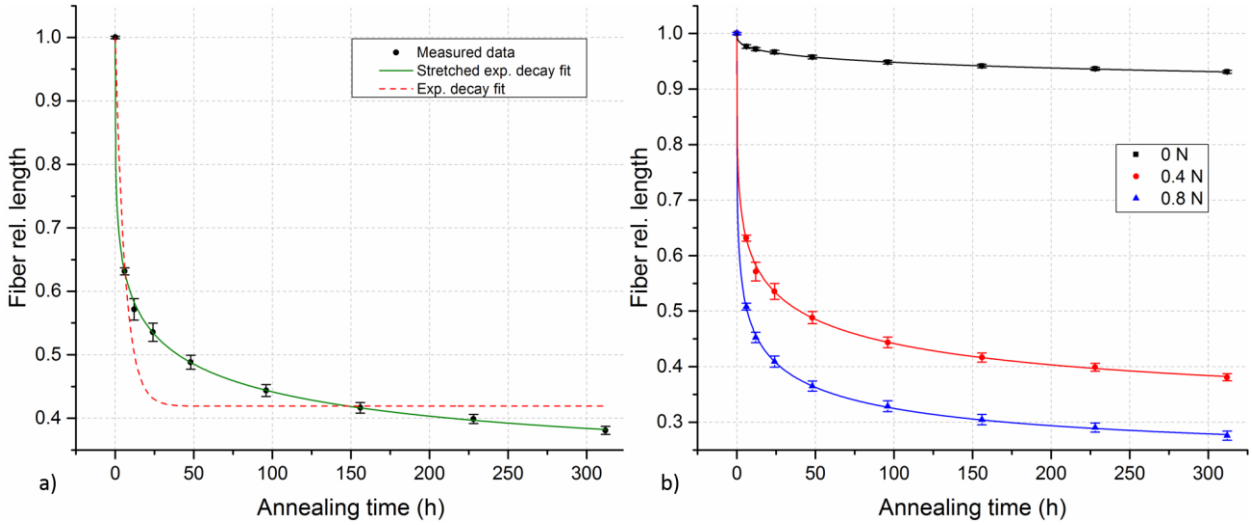

Figure 2. (a) Measured relative length evolution of PMMA fiber (drawn at 0.4 N) fitted with simple and stretched exponential decay functions. (b) Comparison of annealing behavior of fibers drawn under different drawing force. All presented data is for annealing at 95 °C and 40 % RH.

From Figure 2a and data in Table 1, it is apparent that assuming simple exponential decay relaxation may lead to severe underestimation of the degree and evolution of induced shrinkage. Compared to simple exponential decay, the stretched exponential decay function is characterized by faster initial decay for $t < t_0$ and longer and slower tail for $t > t_0$. The effect gets more pronounced as g decreases. From the point of view of fiber/sensor climatic stability, this has rather unfavorable consequences. Firstly, the very rapid initial shrinkage rate makes fibers more prone even to short-term spikes/fluctuations in climatic conditions. Secondly, the longer tail means it takes much longer until the fiber can be considered stable at a certain temperature. Several authors perform short-term annealing of fibers in order to stabilize their geometrical parameters at elevated temperatures. However, our results show that fiber shrinkage is still apparent even for annealing times longer than 10 days.

	Simple exponential decay fit		**Stretched exponential decay fit**	
	Value	**Standard error**	**Value**	**Standard error**
L_0	0.42	0.02	0.32	0.01
L_{An}	0.58	0.02	0.68	0.01
t_0	6.2	0.9	15	2
g	1	0	0.28	0.01

Table 1. Summary of fitted parameters describing annealing behavior from Figure 2a.

Fiber annealing is essentially a relaxation of molecular alignment within the fiber. It is therefore natural to expect that the fiber annealing behavior depends on the initial degree of its molecular alignment. Figure 2b compares the annealing behavior of all three fiber types drawn under different conditions. The increase in induced shrinkage with rising drawing force is clearly visible and in agreement with observations of Ishigure et al. for large-diameter multimode graded-index POFs for data transmission applications [5]. Fiber drawn under extremely low drawing force possesses almost no molecular alignment and its properties are similar to those of bulk isotropic material. Since its molecular arrangement is very close to the equilibrium state, only minimal shrinkage is observed even at temperatures approaching T_g. On the other hand, fiber drawn at fairly high 0.8 N shrinks almost to half

of its original length after just 6 hours at 95 °C and 40 % RH. Fiber drawing at higher force (stress) values is associated with a higher degree of alignment. Aligned molecules then hold higher shrinkage potential as they are trying to return to their original state of random entanglement. Determination of alignment degree from fiber drawing force is not straightforward because it is sensitive to various drawing conditions and their fluctuations. The situation can be even more complicated if a multi-step drawing procedure is employed [13], when a certain level of molecular alignment is introduced already during the cane drawing. In order to get a more objective measure of the fibers' initial degree of molecular alignment, we use the fiber length relaxation ratio R_L. It is a ratio of fiber length before and after complete annealing when full relaxation of the polymer molecules was achieved. After completing a 312 hour annealing cycle at 95 °C and 40 % RH, fiber samples were gradually heated up to 170 °C until no more fiber shrinkage was observed. After cooling, sample lengths were measured again and R_L was calculated to be 1.8 ± 0.1, 12.7 ± 0.2 and 15.1 ± 0.1 for fibers drawn at 0 N, 0.4 N and 0.8 N, respectively. The length relaxation ratio can be also viewed as a total shrinkage potential. The calculated R_L illustrates that the drawing force parameter does not fully characterize the state of the fiber internal molecular structure after the drawing process. It also explains why the difference between the behavior of fiber drawn at 0.4 N and 0.8 N is smaller than one would infer from the drawing force values. Nevertheless, presented results clearly show that fibers prepared at high drawing force are the most unstable ones exhibiting large shrinkage and their use should be avoided if operation at elevated temperatures is expected. On the other hand, drawing under extremely low forces seems to be the most suitable with regard to the fiber climatic stability. However, other factors related to the desired mechanical properties need to be considered as will be discussed later in the work.

Even though we avoid any direct quantitative analysis of fitted parameters, it is worth noting that a consistent trend was observed over the collected data, with t_0 and g decreasing with growing drawing force (molecular alignment). One might then speculate that the drawing process increases the heterogeneity of molecular arrangement in the fiber. This would be in agreement with the description offered by Buckley et al. [4], where two competing mechanisms take place during the drawing process. The fiber drawing process can be imagined as a stretching of a mass of loosely tangled strings. As a result of this longitudinal pulling, a large portion of the molecules is getting preferentially aligned along the stretching direction. At the same time, there are also regions where molecules are becoming even more tightly entangled as the different parts of the same molecules are being pulled away into the aligned regions. With respect to the fiber annealing process, molecules within aligned regions can slide past each other relatively easily, giving rise to faster relaxation and shorter annealing decay times. On the other side of the decay time spectra are highly entangled regions. Polymer chains in highly entangled regions can barely slide past each other, thus restraining movement of involved molecules associated with longer decay times. Increase in the fiber drawing force is then associated not only with the rising shrinkage potential, but also with the faster shrinkage rate and more heterogeneous nature. Besides affecting the annealing behavior, increased heterogeneity may influence fiber optical properties as well. The microscopic heterogeneities in the molecular structure might act as scattering centers increasing fiber optical losses. However, deeper study into the topic would be required in order to confirm the hypothesis.

5.2 Temperature and humidity

Molecular alignment can be viewed in terms of residual stress frozen in the fiber after rapid cooling during the manufacturing process. Even the fibers with the high degree of alignment, far from

the equilibrium state, are considered stable at room temperatures, since the molecular movement is prohibited at temperatures well below the T_g of PMMA. Heat supplied to the fiber at elevated temperatures might be viewed as a sort of activation energy enabling molecular movement. Since aligned molecules are generally less intertwined and can slide past each other more easily, lower energies (temperatures) are sufficient to activate their movement. Figure 3a shows the evolution of relative length of the 0.4 N fiber during the 156 hour annealing process for different annealing temperatures. Even moderately elevated temperatures are sufficient to activate the relative movement of highly aligned molecules. This movement is associated with the fiber shrinkage as the molecules are trying to restore their equilibrium state of random entanglement. The degree of molecular entanglement gradually increases during the annealing process, eventually reaching the point when the supplied thermal energy is not sufficient enough to sustain further molecular movement and the fiber shrinkage saturates. However, fiber may still possess a considerable degree of molecular alignment and further shrinkage can be induced at higher temperatures. In practice it means, that even when the fiber was pre-annealed for sufficiently long time, it can be considered stable only at temperatures up to the utilized annealing one. One has to be even more careful, when only short-term annealing is performed.

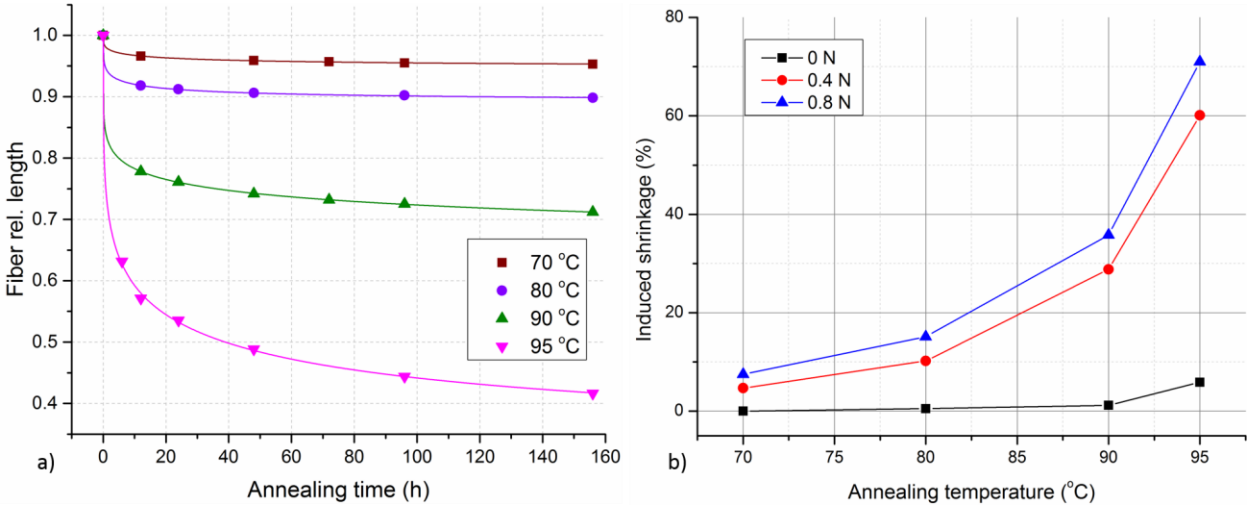

Figure 3. (a) Relative length evolution of fiber drawn at 0.4 N during 156 hour annealing procedure performed at various temperatures. (b) Temperature dependence of fiber shrinkage induced after 156 hour annealing cycle for all investigated fiber types. Relative humidity was fixed at 40 % for all presented measurements.

Figure 3b depicts the induced shrinkage as a function of annealing temperature for all three types of studied fibers and illustrates the superior stability of fibers drawn at lower force values. The fiber drawn under 0 N can be considered stable at temperatures up to 90 °C, where shrinkage of only about 1 % was observed after 156 hours. On the other hand, fiber drawn at 0.8 N exhibits significant shrinkage reaching 10 % already at 70 °C. Moreover, induced shrinkage increases rapidly with rising temperature making the highly aligned fibers even more prone to the annealing effects. The degree of longitudinal shrinkage reaches 70 % at 95 °C for the sample drawn at 0.8 N. At the same time, even the sample drawn at 0 N displays a significant length reduction at this temperature, despite possessing only minimal molecular alignment. This indicates that temperatures between 90 °C and 95 °C can be considered as a more general limit for PMMA drawn fibers with regard to their geometrical stability. Such high temperatures are to be avoided anyway, as they are approaching the T_g value for bulk isotropic PMMA.

The temperature dependence of the annealing process is rather intuitive. However, the situation is further complicated by other climatic factors, particularly relative humidity, which has not been realized in the POF community before. Figure 4a shows the annealing behavior of the fiber drawn at 0.4 N during three separate annealing procedures performed at the same annealing temperature of 90 °C, but under the different level of relative humidity. The results reveal a dramatic influence of RH on the fiber annealing process. Humidity effect on the total fiber shrinkage induced after 156 hour annealing cycle is further depicted in Figure 4b for all three studied fiber types prepared under the different drawing force. The degree of induced shrinkage seems to be rising with the growing RH value. For the fiber drawn at 0.8 N, changing the relative humidity level from 10 % to 70 % results in more than twofold increase of the induced fiber shrinkage, from roughly 20 % to over 70 %. Even for the fiber drawn at 0 N, for which only minimal shrinkage (< 1 %) was measured at 10 % RH, significant length decrease reaching 10 % was observed upon RH increase to 70 %. The observed behavior can be attributed to the plasticizing effect of water molecules on the polymer structure. PMMA, along with many other polymers, exhibits affinity for water, absorbing up to 2 % water content at 23 °C [21]. Water molecules absorbed into the polymer structure of the fiber act as a plasticizer lowering its T_g value [22]. This effectively increases the mobility of polymer molecules and the fiber experiences larger shrinkage analogically to when the annealing temperature is raised.

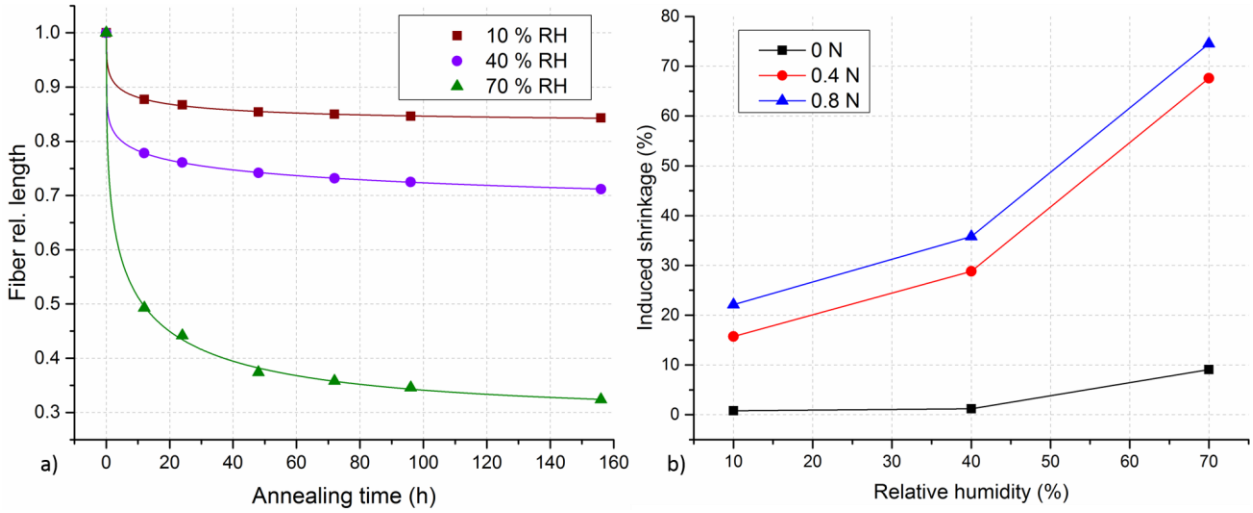

Figure 4. (a) Relative length evolution of fiber drawn at 0.4 N during 156 hour annealing procedures performed at various RH levels. (b) Humidity dependence of total fiber shrinkage after 156 hour annealing cycle for all investigated fiber types. Annealing temperature was fixed at 90 °C for all presented measurements.

Furthermore, the shrinkage promoting effect of humidity seems to extend down to the room temperatures, where the fiber parameters are otherwise considered stable. Table 2 summarizes the relative length change ΔL of the all three fiber types induced solely by the water absorption. In this case, eight samples of each fiber type with an initial length of 2 m were coiled and left in a container filled with distilled water for a period of 24 hours. The sample length was measured again immediately after they were taken out of the water bath and briefly dried with a paper towel. Since water absorption into polymers is accompanied by material swelling, fibers were left for another 24 hours in order to stabilize back at the original room conditions (22-24 °C, 44-48 % RH) and their length was measured again. Subtle but significant difference in the responses of the different fibers was observed. In case of the fiber drawn at 0 N, a length increase of 0.28 ± 0.01 % was recorder right after the 24 hour soaking period.

Upon drying at the room conditions the fiber returned to its initial length. Such behavior is associated with simple swelling of polymer by absorption of water molecules without any permanent change in the fiber molecular structure. Contrary to that, no significant swelling is observed for the fiber drawn at 0.8 N right after the water bath. After desorption of excess water from the fiber at the room conditions, permanent shrinkage of -0.13 ± 0.02 % was recorded. This indicates that presence of water molecules in the polymer structure is sufficient to induce relaxation of highly aligned molecules even at room temperatures. Even though the effect may appear fairly low when only fiber length change is considered, it represents considerable change of the measured values in the case of POF-based sensors. For an FBG written at 1550nm in PMMA fiber, shrinkage of -0.13 % amounts to a 2.015 nm down-shift of the FBG wavelength considering only the geometrical change of the grating period. This wavelength shift is equivalent to a fairly high strain drop of approximately 1.44 mε or a temperature increase in excess of 72 °C, considering 1.4 pm/με strain and 28 pm/ °C temperature sensitivity, respectively [23]. This means one needs to consider suitable pre-annealing of the fiber not only for operation at elevated temperatures but also when operation in high-humidity or water environments is foreseeable. We would also like to note that the results indicate a difference in the humidity response of the fibers. If the length of the dry fiber 24 hours after removal from the water bath is considered as a new stable state (after relaxation), then the length of the wet fiber immediately after the water bath represents the state of saturated water absorption into the fiber. From the relative difference between these states, one can see that water induced swelling appears to be smaller for fibers with a higher degree of molecular alignment. This might be of interest for applications where polymer optical fiber Bragg gratings are exploited for water (humidity) sensing.

	ΔL [%]		
	0 N	**0.4 N**	**0.8 N**
wet	0.28 ± 0.01	0.09 ± 0.03	0.00 ± 0.02
dry	0.01 ± 0.02	-0.09 ± 0.02	-0.13 ± 0.02

Table 2. Relative length change of the fibers prepared at different drawing force immediately after 24 hour water bath (wet) and after additional 24 hour drying period (dry).

5.3 Mechanical properties

As mentioned earlier, fiber geometrical stability is not the only factor that needs to be considered during the optimization of fiber drawing conditions. After all, one of the main motivation factors for utilization of POFs are their advantageous mechanical properties, such as increased elasticity or lower stiffness. Strong dependence of virtually all basic fiber mechanical properties on drawing conditions has been clearly shown in the different studies [3–6]. The drawing stress (tension) associated with the drawing force and the fiber final diameter turns out to be the most decisive parameter. The general trend for the majority of basic parameters such as yield stress and strain, Young's modulus and tensile strength is that they grow monotonically with increasing drawing stress. The situation regarding the fiber ultimate strain is a bit more peculiar. An initial increase of maximal achievable elongation is followed by the gradual decrease after a certain threshold of used drawing stress is reached. Once again, the explanation for the observed behavior can be found on the structural level in the competitive molecular reorganization mechanisms described before. With increasing drawing stress, the tensile related properties of the fiber are being defined by an increasing proportion of aligned molecules with high strength and stiffness. Aligned molecules can move past each other more easily which accounts for

the initial growth of the fiber ultimate strain when the fiber drawing stress is increased. However, after a certain point, movement of these molecules becomes prohibited by an increasing number of highly entangled regions and the fiber ultimate strain starts to drop again. This is crudely illustrated in Figure 5a depicting typical stress-strain curves of our three fiber types manufactured under different drawing force. Fiber drawn at 0 N possesses only minimal degree of molecular alignment and exhibits brittle straining behavior similar to the bulk isotropic material. It has a fairly low ultimate strain limit and in general breaks very easily. Fiber drawn at 0.4 N has a more advantageous, higher ultimate strain limit reaching 25 %. However, increasing drawing force further to 0.8 N already leads to the decrease of the maximal applicable strain. The fiber exhibits more brittle characteristics, but with higher strength. Fibers drawn at extremely low tensions might be more attractive from the point of view of climatic stability, but need not be the most suitable ones with regard to the broader practical requirements.

Achieving advantageous mechanical properties desired for many sensing applications requires introduction of a certain degree of molecular alignment. In this case, a relaxation induced change of the fiber mechanical parameters ought to be considered with respect to the foreseeable operating conditions of the sensor as well. Figure 5b illustrates the effects of the fiber annealing on its straining behavior. In this context, thermal annealing can be viewed as an inverse process to the fiber drawing, leading to the relaxation, as opposed to the introduction, of molecular alignment. Compared to an increase of the fiber drawing stress, an analogous but opposite effect can be observed with the increasing degree of induced relaxation. For the fiber drawn at 0.8 N, steady decrease of fiber strength and Young's modulus was observed up to the maximal annealing temperature used (95 °C). While fiber ultimate strain increases up to the annealing temperature of 90 °C, further increase to 95 °C already induces a significant drop of maximal strain values and the fiber becomes more brittle. The annealing-induced change of the mechanical properties is not likely to severely limit fiber usability in the sensing applications. Considering that most of the sensing methods are limited to the elastic region, there is a broad range of molecular alignment degree that is sufficient to ensure superior elasticity of POFs. Only subjecting the fiber to rather extreme conditions might lead to more serious deterioration of the fiber mechanical performance. However, changes of the fiber straining behavior in the elastic region, in particular decrease of Young's modulus, might be relevant for sensor reliability in stress-based sensing schemes.

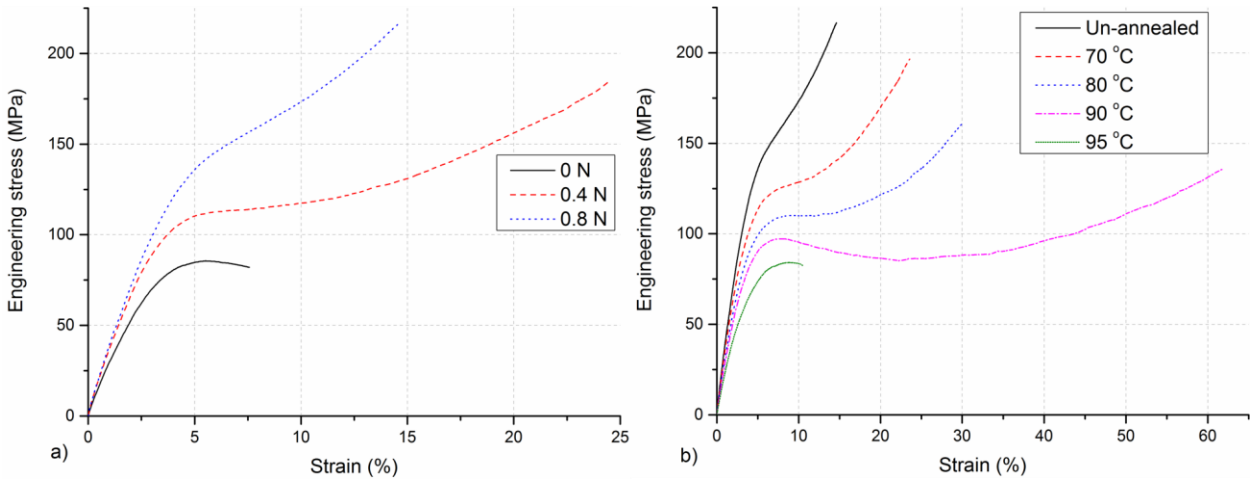

Figure 5. Typical stress-strain curves of un-annealed fibers prepared under different drawing stress (a) and for fiber drawn at 0.8 N annealed at different temperatures and 40 % RH for 156 hours (b).

6. Conclusions

Molecular alignment in drawn polymer fibers and its relaxation was investigated with respect to the climatic stability of polymer optical fibers for sensing applications. Heterogeneous dynamics of the annealing process was revealed and its rather unfavorable consequences for the fiber/sensor stability were discussed. Annealing-induced fiber shrinkage was shown to be strongly dependent on the initial degree of molecular alignment in the fiber and climatic conditions. Besides the expected temperature dependence, also strong humidity dependence of the annealing process was demonstrated. The results strongly suggest that fibers with a low degree of molecular alignment should be used if sensor operation at elevated temperature or humidity is expected. On the other hand, a certain degree of molecular alignment is required to maintain the advantageous mechanical properties of polymer optical fibers. In this case, suitable controlled pre-annealing should be performed with respect to the foreseeable operating conditions. However, special attention needs to be paid when choosing the suitable pre-annealing conditions due to the heterogeneous nature and complexity of the annealing process, especially with regard to sensor long-term stability.

Acknowledgement

The research leading to these results has received funding from the People Programme (Marie Curie Actions) of the European Union's Seventh Framework Programme FP7/2007 2013/ under REA grant agreement n° 608382. Pavol Stajanca thanks to Mathias Breithaupt and Sven Münzenberger for assistance with experiment.

References

[1] O. Ziemann, J. Krauser, P.E. Zamzow, W. Daum, POF handbook: Optical short range transmission systems, second ed., Springer, Berlin, 2008.

[2] K. Peters, Polymer optical fiber sensors—a review, Smart Mater. Struct. 20 (2010) 013002.

[3] D. Bosc, C. Toinen, Tensile mechanical properties and reduced internal stresses of polymer optical fiber, Polym. Compos. 14 (1993) 410–413.

[4] C.A. Buckley, E.P. Lautenschlager, J.L. Gilbert, Deformation processing of PMMA into high strength fibers, J. Appl. Polym. Sci. 44 (1992) 1321–1330.

[5] T. Ishigure, M. Hirai, M. Sato, Y. Koike, Graded-index plastic optical fiber with high mechanical properties enabling easy network installations II, J. Appl. Polym. Sci. 91 (2004) 410–416.

[6] C.H. Jiang, M.G. Kuzyk, J.L. Ding, W.E. Johns, D.J. Welker, Fabrication and mechanical behavior of dye-doped polymer optical fiber, J. Appl. Phys. 92 (2002) 4–12.

[7] P. Ji, A.D.Q. Li, G.-D. Peng, Transverse birefrigence in polymer optical fibre introduced in drawing process, in: Proc. SPIE 5212, Linear Nonlinear Opt. Org. Mater. III, 2003.

[8] M.K. Szczurowski, T. Martynkien, G. Statkiewicz-Barabach, W. Urbanczyk, L. Khan, D.J. Webb, Measurements of stress-optic coefficient in polymer optical fibers, Opt. Lett. 35 (2010) 2013–2015.

[9] M. Sato, T. Ishigure, Y. Koike, Thermally stable high-bandwidth graded-index polymer optical fiber, J. Light. Technol. 18 (2000) 952–958.

[10] W. Yuan, A. Stefani, M. Bache, T. Jacobsen, B. Rose, N. Herholdt-Rasmussen, et al., Improved thermal and strain performance of annealed polymer optical fiber Bragg gratings, Opt. Commun. 284 (2011) 176–182.

[11] K.E. Carroll, C. Zhang, D.J. Webb, K. Kalli, A. Argyros, M.C. Large, Thermal response of Bragg gratings in PMMA microstructured optical fibers, Opt. Express. 15 (2007) 8844–8850.

[12] I.P. Johnson, D.J. Webb, K. Kalli, Utilisation of thermal annealing to record multiplexed FBG sensors in multimode microstructured polymer optical fibre, in: Proc. SPIE 7753, 21st Int. Conf. Opt. Fiber Sensors, 2011: p. 77536T.

[13] M.C.J. Large, L. Poladian, G.W. Barton, M.A. van Eijkelenborg, Microstructured polymer optical fibres, Springer, 2007.

[14] E. Industries, Plixiglas datasheet, (n.d.). http://www.plexiglas.de/product/plexiglas/Documents/PLEXIGLAS/211-12-PLEXIGLAS-Tubes-Rods-en.pdf.

[15] J. Olszewski, P. Mergo, K. Gasior, W. Urbanczyk, Highly birefringent microstructured polymer fibers optimized for a preform drilling fabrication method, J. Opt. 15 (2013) 075713.

[16] M.N. Berberan-Santos, E.N. Bodunov, B. Valeur, Mathematical functions for the analysis of luminescence decays with underlying distributions 1. Kohlrausch decay function (stretched exponential), Chem. Phys. 315 (2005) 171–182.

[17] L. Berthier, G. Biroli, J.-P. Bouchaud, L. Cipelletti, W. van Saarloos, Dynamical Heterogeneities in Glasses, Colloids, and Granular Media, Oxford University Press, 2011.

[18] M.D. Ediger, Spatially heterogeneous dynamics in supercooled liquids., Annu. Rev. Phys. Chem. 51 (2000) 99–128.

[19] I.M. Ward, ed., Structure and properties of oriented polymers, Springer Science & Business Media, 2012.

[20] R. Richert, A. Blumen, eds., Disorder effects on relaxational processes: glasses, polymers, proteins, Springer Science & Business Media, 2012.

[21] J. Brandrup, E.H. Immergut, A. Abe, D.R. Bloch, eds., Polymer handbook (Vol. 89), Wiley, New York, 1999.

[22] H. Levine, L. Slade, Water as a plasticizer : physico-chemical aspects of low-moisture polymeric systems, in: Water Sci. Rev. 3 Water Dyn., 1988: pp. 79–185.

[23] D.J. Webb, Polymer Fiber Bragg Grating Sensors and Their Application, in: G. Rajan (Ed.), Opt. Fiber Sensors Adv. Tech. Appl., CRC Press, 2015: pp. 257–276.